to be published in
Optoelectronic Integration on Silicon
edited by David J. Robbins and Ghassan E. Jabbour,
Proceedings of SPIE (Photonic West, San Diego 2003)

A review of the various efforts to a silicon laser

L. Pavesi[a]
INFM and Dipartimento di Fisica
Università di Trento
Via Sommarive 14, 38050 Povo(Trento), Italy

ABSTRACT

The various approaches to a silicon laser are here critically reviewed: bulk Silicon, Silicon nanocrystals, Erbium coupled Silicon nanocrystals, Silicon/Germanium quantum cascade structures, Silicon intracenter recombinations for THz emission. It is predicted a bright future to silicon.

Keywords: silicon laser, stimulated emission, nanocrystals, erbium, silicon germanium, quantum cascade, intracenter recombinations

1. INTRODUCTION

Silicon is the electronic material *per excellence*. Integration and economy of scale are the two keys ingredients for the silicon technological success. Silicon has a band-gap of 1.12 eV that is ideal for room temperature operation and an oxide SiO_2 that allows the processing flexibility to place today more than 10^8 devices on a single chip. The continuous improvements of silicon technology has made possible to grow routinely 200 mm single silicon crystals at low cost and even larger crystals are now under development. The high integration levels reached by the silicon microelectronic industry have permitted high-speed device performances and unprecedented interconnection levels.[1] The present interconnection degree is sufficient to cause interconnect propagation delays, overheating and information latency between single devices. The overcome of this *interconnection bottleneck* is together the main motivation and opportunity for the present-day silicon microphotonics, where attempts to combine photonic and electronic components on a single Si chip or wafer are strongly pursued. In addition, photonics aims to combine the power of silicon microelectronics with the advantages of photonics. With photonics into the chip, the continuous increase of performances predicted by Moore's law can be faced.

Silicon microphotonics has boomed in recent years.[2-5] Almost all the various photonics devices have been demonstrated: e.g. silicon based optical waveguides with extremely low losses and small curvature radii,[3] tuneable optical filters, fast switches (ns),[6] and fast optical modulators (GHz),[7] fast CMOS photodetectors,[8] integrated Ge photodectors for 1.55 μm radiation.[5,9] Micromechanical systems or photonic crystals have been demonstrated and switching systems are already commercial. On the other hand, the main limitation of silicon photonics is the lack of any practical Si-based light sources: either efficient light emitting diodes (LED) or a Si lasers.

Silicon is an indirect band-gap material, light emission is a phonon-mediated process with low probability (spontaneous recombination lifetimes in the ms range). In standard bulk silicon, competitive non-radiative recombination rates are much higher than the radiative ones and most of the excited e-h pairs recombine non-radiatively. This yields very low internal quantum efficiency ($\eta_i \approx 10^{-6}$) for bulk silicon luminescence. In addition, fast non-radiative processes such as *Auger* or *free carrier* absorption severely prevent population inversion for silicon optical transitions at the high pumping rates needed to achieve optical amplification. Despite of all, during the nineties many different strategies have been employed to overcome these materials limitations.[4] The most successful ones are based on the exploitation of low dimensional silicon where silicon is nanostructured and hence the electronic properties of free carriers are modified by quantum confinement effects. A steady improvement in low dimensional silicon LED performances has been achieved and silicon LEDs are now only a factor of ten out of the severe market requirements.[10,11]

[a] Email: pavesi@science.unitn.it; url: http://science.unitn.it/~semicon/

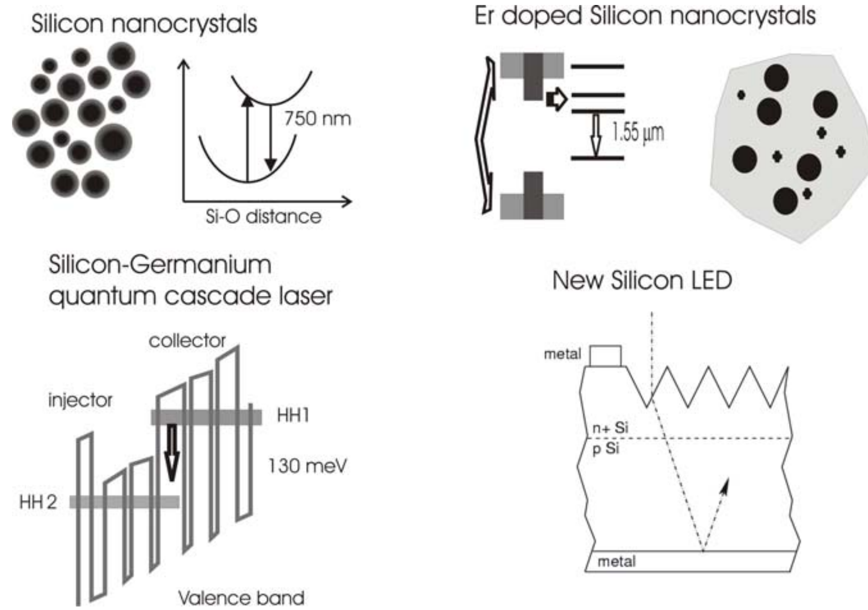

Figure 1. Various approaches proposed to realize a silicon laser.

In addition, recently many breakthroughs have been demonstrated showing that this field is very active and still promising. Figure 1 shows a schematic sketch of the various approaches that are currently followed to build a silicon laser. They differ both for spectral region of emission and for the physics behind. A NATO advanced research workshop was held in Trento at the end of 2002 where all these approaches have been presented and discussed. The results of the workshop have been published, here I will review these works and I refer the interested reader to the published book.[12]

2. BULK SILICON

Silicon is an indirect band gap material, thus the probability for a radiative transition is very low. This is reflected into very long times for radiative recombinations. Due to these long radiative lifetimes, excited free carriers have large probabilities to find non-radiative recombination centres and to recombine non-radiatively. Room temperature emission in bulk silicon with high efficiency has been only observed in ultra pure silicon with the surface passivated by a native oxide where excited carrier lifetimes are dominated by radiative recombination.[13] This idea to increase the quantum efficiency of Si has been followed by two different approaches to develop Si based light emitting diodes.[11,14]

The first approach is based on the results achieved in high efficiency solar cells and on the consideration that within thermodynamic arguments absorption and emission are two reciprocal processes.[11] At first the non-radiative rates are reduced using 1) high-quality Si substrates, float-zone (FZ) being preferred over Czochralski (CZ), 2) passivation of surfaces by high-quality thermal oxide, in order to reduce surface recombination, 3) small metal areas, and 4) high doping regions limited to contact areas, in order to reduce the SRH recombination in the junction region. Then, the parasitic absorption of photons once they have been generated is reduced at minimum. For example, the reabsorption can be minimized by keeping the doping level to moderate values, such as $\sim 1.4 \times 10^{16}$ cm^{-3}. Finally, the extraction efficiency of light from bulk silicon can be enhanced by suitably texturizing the Si surface. The final device structure is shown in Fig. 2. Ref. 11 reports the highest to date power efficiency for Si based LED, approaching 1 %. Electroluminescence spectra of these devices (Fig. 3) are typical for band-to-band recombinations in silicon.

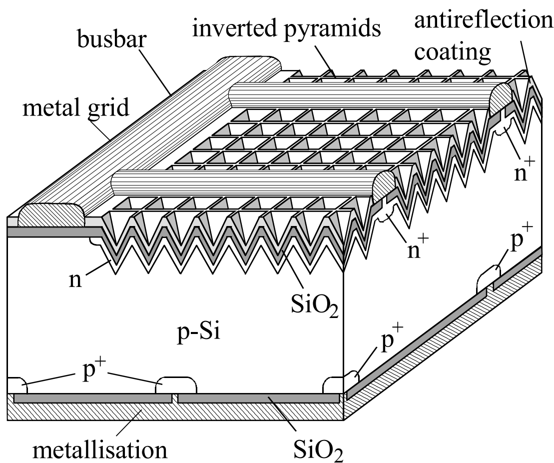

Figure 2. Design of the textured Si light emitting device. After Ref. 11.

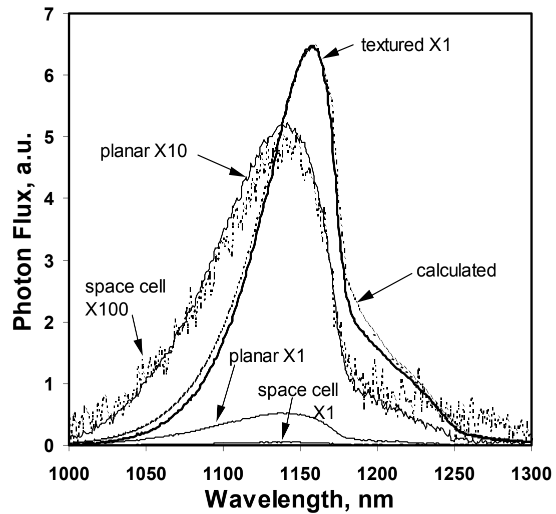

Figure 3. Electroluminescence spectra for textured, planar and baseline space cell diodes under 130 mA bias current at 298 K (diode area 4 cm^2) Calculated values assume a rear reflectance of 96 % . After Ref. 11.

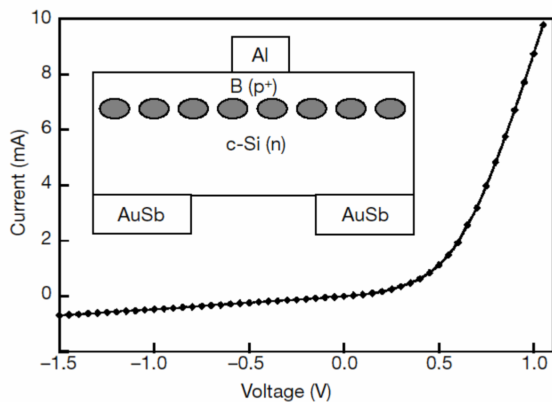

Figure 4. Current-voltage characteristics for the device measured at room temperature. Inset: a schematic of the LED where the grey circles evidenced the region reach in dislocation loops. The top and bottom ohmic contacts are formed by Al and AuSb respectively. The infrared light is emitted through the window left in the bottom contact. After Ref. 14.

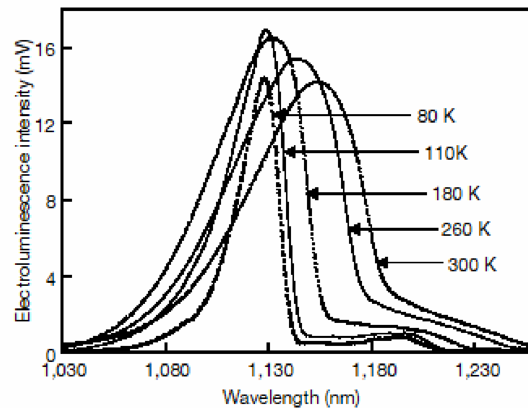

Figure 5. Electroluminescence spectra against wavelength at various temperatures. The device was operated at a forward current of 50 mA for all temperatures. After Ref. 14.

The main drawback of this approach for an integrated light emitting diode is the need of both high purity (low doping) and of texturing which render the device processing not compatible with standard CMOS processing. In addition, to use this approach for a silicon laser some problems can be foreseen in the strong and fast free carrier absorption typical of bulk Si that can prevent reaching the condition for population inversion.[15] Also suitable integration of the active bulk Si into an optical cavity can be a problem.

A somehow different approach was reported in Ref. 14, see Fig. 4 and 5. The idea was again a reduction of the non-radiative channels by exploiting the strain produced by localized dislocation loops to form energy barriers for carrier diffusion. Dislocations form potential pockets close to the junction which block the carriers and enhance radiative decay by localizing them in defect-free regions. The size of dislocation loops was in the range of 100 nm, i. e. not enough to cause a quantum confinement of the carriers, and the loop distances were of the order of 20 nm. The onset of the elec-

troluminescence (EL) at the band edge was observed as the diode turns on under forward bias. No EL was observed under reverse bias. External quantum efficiency of about 1 % are claimed for these LED. The EL spectrum does not present significant differences in lineshape or the peak position compared to that of bulk-Si (Figure 5). A remarkable feature of this device is the high injection efficiency into the confined regions. This is due to the lack of quantum effects. In fact, since the density of states in active zone is large (comparable to bulk value), it is not a limiting factor for the free carrier injection, contrary to quantum confined structures. On the other hand, injection is also smooth because there is no wide band-gap material as confining barrier. Although not explained, this device has the additional and interesting feature of increasing the efficiency with temperature. The positive role of dislocation loops in enhancing luminescence from near surface silicon has been further confirmed by other authors.[16,17] The main problem of this approach for a silicon laser is that it does not remove the two main problems of silicon which prevents population inversion, i. e. Auger recombination[18] and free carrier absorption[15].

Finally a problem is also related to the wavelength of emission of these bulk Silicon LED which is resonant with the silicon band gap: that means that it is very difficult to control the region where the light is channelled in silicon if one want to use these LED as a source for optical interconnects. Light will propagate through the wafer and will be absorbed in unwanted places.

3. SILICON NANOCRYSTALS

Another way to increase the emission efficiency of silicon is to turn it into a low dimensional material and, hence, to exploit quantum confinement effects to increase the radiative probability of carriers. This approach has been pioneered by the work of L. Cahanm which showed that when silicon is partially etched in an HF solution via an electrochemical attack, the surviving structure is formed by small nanocrystals or nanowires which show bright red luminescence at room temperature.[19] This material is called Porous silicon.[20] The explanation of the observed high luminescence internal quantum efficiency was: i) quantum confinement which leads to an enlargement of the band-gap and to an increased recombination probability, ii) the spatial confinement of the free carriers which prevent them to reach non radiative recombination centres, iii) the reduction of the refractive index of the material which increases the extraction efficiency via refractive index matching. This result has motivated many research efforts in order to exploit these properties in LED. The evolution of porous silicon LED performance over the year is reported in Fig. 6.

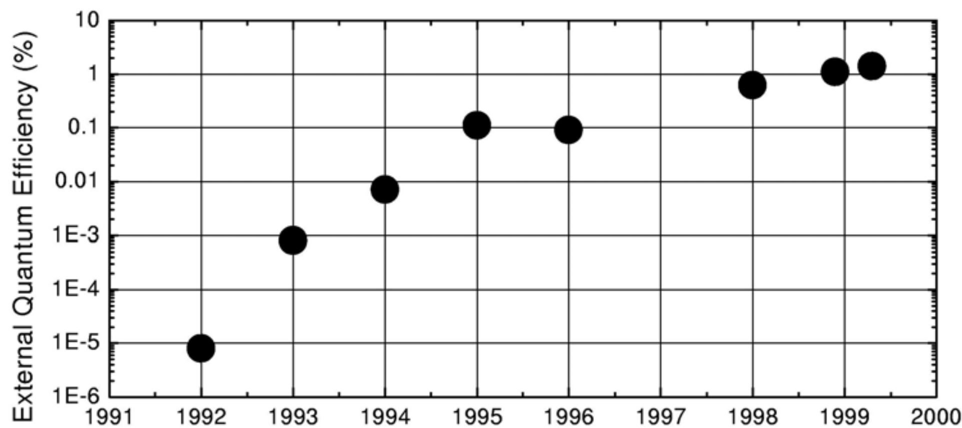

Figure 6. External quantum efficiency of porous silicon LED over the year. The record in efficiency to date is that of Ref. 10.

The porous silicon approach has however a draw-back in the high reactivity of the sponge-like texture which causes the rapid ageing of the LED and an uncontrollable variations of the LED performances with time. In addition, a preliminary study performed in my laboratory does not evidence any optical amplification in porous silicon waveguides except for some positive data, still to be confirmed, in the blue region of the spectrum for some oxidized porous silicon samples grown in Munich by D. Kovalev.

An alternative way is to produce silicon nanocrystals (Si-nc) in a silica matrix to exploit the quality and stability of SiO_2/Si interface and the improved emission properties of low dimensional silicon. Many different approaches have been proposed to form the silicon nanocrystals. The most widely used are based on the formation of sub-stoichiometric silica films, with a large excess of silicon, followed by a high temperature annealing. The annealing causes a phase separation between the two constituent phases, i.e. silicon and SiO_2 with the formation of small silicon nanocrystals. The sizes and density of the Si-nc can be controlled by the deposition and the annealing parameters. Recently, the use of amorphous Si/SiO_2 superlattices has been proposed to control the size distribution. Almost monodispersed size distribution has been demonstrated.[21]

The luminescence properties of Si-nc are very similar to those of porous silicon: a wide emission band is observed at room temperature whose spectral position depends on the Si-nc sizes. In these systems optical gain has been observed.[22-26] Table 1 summarizes the main results and sample parameters from those works where Si-nc related gain has been reported.

TABLE 1. Principal structural and optical parameters of the samples. T refers to the annealing temperature used to form the Si-nc. R_{Si-nc} and ΔR_{Si-nc} are the mean value and the width of the radii distribution of the Si-nc measured by TEM, λ^{PL}_{max} and $\Delta\lambda^{PL}$ the wavelength of the maximum and width of the luminescence emission band, g the measured modal gain coefficient, λ^{g}_{max} the wavelength of the maximum gain, n the refractive index of the samples measured by m-line measurements at 633 nm, Γ the optical confinement factor, ρ the Si-nc density in the sample estimated by X-ray measurements and σ_g the Si-nc gain cross section at 750 nm.

Growth technique	T (^{0}C)	R_{Si-nc} (nm)	ΔR_{Si-nc} (nm)	λ^{PL}_{max} (nm)	$\Delta\lambda^{PL}$ (nm)	g (cm^{-1})	λ^{g}_{max} (nm)	n	Γ	ρ (cm^{-3}) $x10^{18}$	σ_g (cm^2) $x10^{-17}$	REF
Ion implanted	1100	3		830	180	100	750	1.89	0.097	20	5	22
PECVD	1250	2.1	1.2	938	215	60	721	2	0.83	4.6	4.3	23
PECVD	1250	1.7	1.1	906	188	48	751	1.82	0.76	6.3	3.6	23
Si deposition	1150	3-4		790	180	6	720					24
Colloidal		1		390		$1.5x10^{3-4}$ *	400	2				25
Colloidal		2.9				$7x10^4$ *	610	2		70,000		26
Ion implanted	1100			440								27
Magnetron sputtering		3		660	150	100	800		1		0.2	28
Ion implanted	1100	5		870		33	922					29

* This value refers to the material gain

Almost all the authors agree on the fact that the gain is due to localized state recombination either in the form of silicon dimers[25-27] or in the form of Si=O bonds formed at the interface between the Si-nc and the oxide or within the oxide matrix[22-24,30]. The suggested scheme to explain population inversion and, hence gain, is a four level model where a large lattice relaxation of the localized centre gives rise to the four levels (see Fig. 7 and 8).

Optical gain in Si-nc has been revealed either as a superlinear increase of the luminescence intensity,[25,27] or as the measurements of amplified spontaneous emission in a waveguide geometry (see Fig. 9),[22-24,28-30] or as probe amplification in transmission experiments under high pumping excitation,[22] or as collimated and speckled patterned emissions from Si-nc.[26] Some concerns have been raised about the methods used to measure gain (see in Ref. 12 and 31). Very interesting information can be achieved by time resolved experiments of the amplified spontaneous emission from Si-nc in a waveguide geometry.[23,24,30] Figure 10 reports the decay lineshape of the amplified spontaneous emission both as a function of the pumping fluencies (Fig. 10a) or as a function of the excited length (Fig. 10b). In addition to the usual slow recombination of Si-nc (µs range), a fast contribution (ns time scale) is observed which grows up either by increasing the fluence or by increasing the excitation length. This last observation rules out Auger recombination as the cause of the fast component because of its strongly non-linear dependence on the photo-excited carrier concentration, which in Fig. 10b is constant for all the various lengths. The origin of the fast component in these Si-nc is stimulated emission. This is supported also by other experimental data.

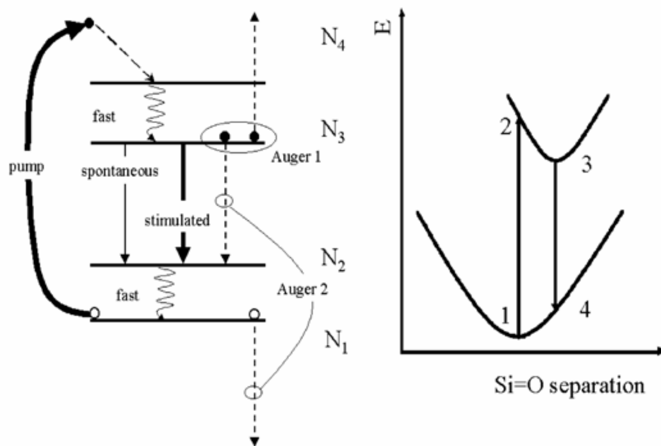

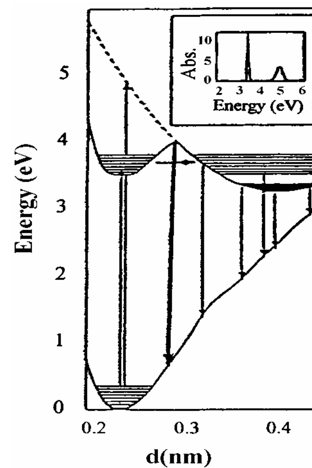

Figure 7. (Left) Effective four level system that models qualitatively the recombination dynamics under gain conditions. Two different kinds of Auger recombinations are considered and can be studied on the basis of the rate equations of the relaxation dynamics. (right) Schematic of the energy configuration diagram of the silicon nanocrystals in an oxygen rich matrix. Localised radiative states are formed inside the nanocrystal band-gap by the interface oxygen atoms. The excited nanocrystal state can occur at a different lattice coordinate with respect to the ground state. From Ref. 30.

Figure 8. Interatomic potential of the dimmers in 1.03 nm crystallites showing the ground and the first excited electronic states, along with the pathways for excitation and emission. The inset is the transition probability in absorption. From Ref. 25.

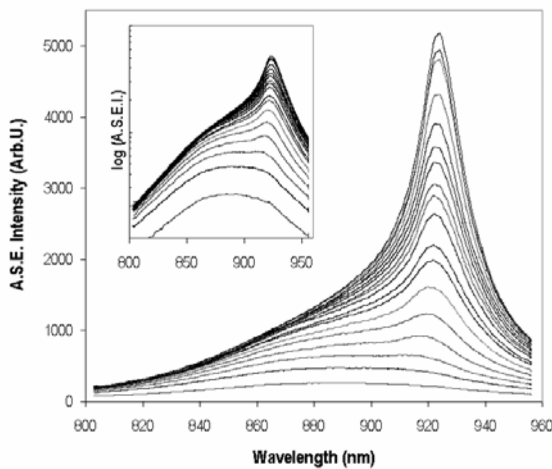

Figure 9. Room temperature amplified spontaneous emission (A.S.E.) spectra of the sample S2 in dependence on the strip length starting with 50 μm for the low intensity spectrum with a constant increase by 50 μm up to 700 μm for the high intensity spectrum. The stimulated emission appeared at 922 nm. The inset shows the same, but using logarithmic value for the A.S.E. intensity. From Ref. 29

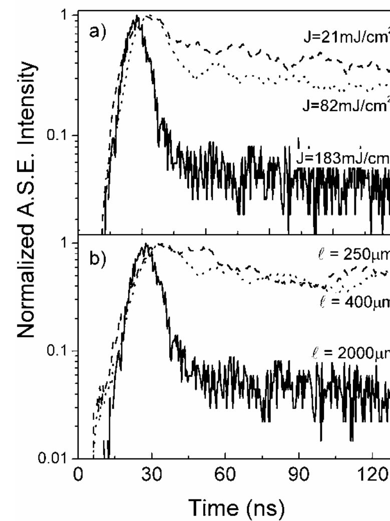

Figure 10. (panel a) Normalised Amplified Spontaneous Emission (A.S.E.) measured under VSL geometry with a pumping length ℓ=2mm at the different pumping fluences reported on the figure. The measured sample is a 42% at of Si annealed at 1250° for 1h. Excitation wavelength was 355nm. (panel b) Here the effect of the pumping length ℓ on the fast A.S.E. dynamics is shown. The pumping fluence is fixed at 183mJ/cm^2 and only the pumping length is varied according to the values reported on the figure.

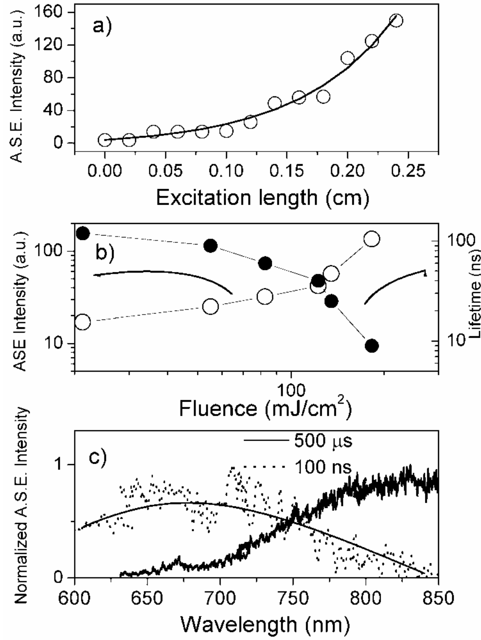

Figure 11. (panel a) Points: Amplified Spontaneous Emission (A.S.E.) peak intensity at 760 nm versus the excitation length at a pump fluence of $200 mJ/cm^2$. Full line: fit of the experimental data with the one-dimensional amplifier model which yields a net modal gain values of 12 ± 3 cm^{-1}. (panel b) open circles: A.S.E. peak intensity of the fast component versus the pumping fluence. Black discs: 1/e lifetime of the A.S.E. decay as a function of the pumping fluence. Excitation length was approximately ℓ=2mm. (panel c) Amplified spontaneous emission (A.S.E.) spectra measured for a fixed excitation length ℓ =2mm and pumping fluence of 200 mJ/cm^2 for two different integration time windows. Dotted line 100 ns after the excitation while the full line 500 µs. All the data in this figure have been taken with an excitation wavelength of 355nm.

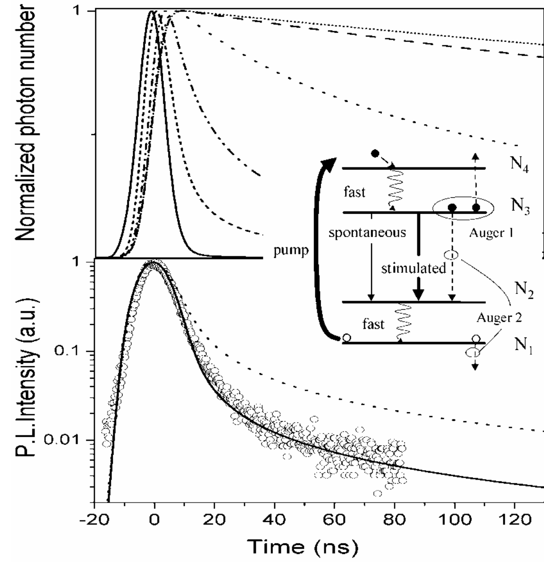

Figure 12. (Top panel) Simulations of the normalised PL intensity as a function of the incident photon flux ϕ_P. The peak of the incident photon flux ϕ_P was varied between 10^{16} and 10^{24} photons $s^{-1}cm^{-2}$. The main parameters used in the simulation were the pump absorption cross section $\sigma_P=10^{-14}cm^2$, the emission cross section $\sigma=10^{-17}cm^2$, the active centers concentration N=8x10^{18} cm^{-3}, the spontaneous emission factor β=4.5x10^{-4}, the optical losses $\alpha=25cm^{-1}$. No Auger recombination has been considered here. (Bottom panel) PL decay (open circles) of Si-nc produced by PECVD deposition of a 46% at of Si annealed at 1250° for 1h. The solid line is a simulation obtained with the same parameters as in the top panel plus an effective Auger coefficient C_A=10x10^{-10} cm^{-3} s^{-1} (peak Auger lifetime of 3ns) and a pump photon flux of 5x10^{22} photons $s^{-1}cm^{-2}$. The dashed line is a simulation where no stimulated emission was present, only Auger recombination. In this case an Auger coefficient of C_A=2x10^{-8} cm^{-3} s^{-1} (peak Auger lifetime of 90 ps) is needed.

Figure 11a reports the exponential increase of the fast component intensity as a function of the photoexcited volume (which yields a net modal gain of 11 cm^{-1} under these pumping conditions). Figure 11b shows a clear fluence threshold over which the amplified spontaneous emission increases superlinearly with the fluencies and the decay lifetime of the emission decreases to a few ns. Figure 11c shows that the spectral shape of the fast component is different than the one of the slow component reflecting the typical blue shift of the gain band with respect to the luminescence which support the four level model of Fig. 7. In addition this model is also able to reproduce the decay of the luminescence at high fluencies for Si-nc as demonstrated in Fig. 12. In the simulation of Fig. 12 both stimulated emission and Auger recombination are taken into account. At the peak fluence the lifetimes associated to these to process are only slightly different. It is also this delicate interplay between Auger recombination and stimulated emission that governs the optical gain in Si-nc. As discussed in Ref. 30 the Si-nc density should be large enough to yield a significant optical gain. This means that not in all Si-nc samples optical gain can be achieved. It is interesting to note that the data of Fig. 12 cannot be fitted with only Auger recombinations, even with peak Auger lifetimes as short as 90 ps. The contribution from stimulated emission is needed to accurately reproduce the luminescence decay.

The Si-nc system is very promising to achieve a laser. Indeed other key ingredients for a laser have been demonstrated. Vertical optical micro-cavities based on a Fabry-Perot structure with mirrors constituted by Distributed Bragg Reflectors (DBR) and where the central layer is formed by Si-nc dispersed in SiO_2 have been already fabricated.[32] Figure 13 shows an example of such Si-nc microcavities with a quality factor of 500 where it is demonstrated a record line narrowing of the emission down to 1.5 nm and a 40 times stronger peak intensity for the microcavity sample than for the reference.[32] The presence of thick SiO_2 layer needed to form the DBR can be a problem for electrical injection when current has to flow through the DBR. Later injection schemes can avoid these problems. On the other hand the electrical injection into the Si-nc is a delicate task by itself.[33] Bipolar injection is extremely difficult to achieve. Despite some claims, most of the reported Si-nc LED are impact ionisation devices: electron-hole pairs are generated by impact ionisation by the energetic free-carriers injected through the electrode. By exploiting impact ionisation Si-nc LED have been demonstrated with electroluminescence spectra overlapping luminescence spectra, onset-voltage as low as 5 V and efficiencies in excess of 0.1%.[34] Some unconfirmed claims of near-laser action of Si-nc LED have appeared in the literature.[35,36]

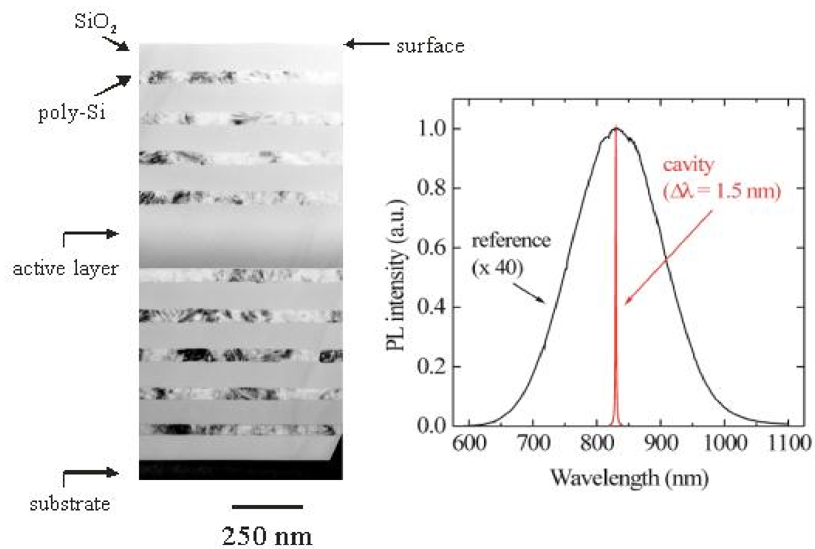

Figure 13 TEM image of a Si-nc microcavities (the DBR are formed by stacking $\lambda/4$ thick layers of Si and SiO_2) and luminescence spectra of Si-nc reference sample and Si-nc in the cavity. From Ref. 32.

Main aspects that require further work are: i) the optimized material parameters and waveguide geometry (see the spread of the values in Table 1), ii) pump and probe experiments in waveguide configuration, iii) the role of nanocrystal interaction, iv) the role and composition of the SiO_2 embedding matrix, v) the precise nature of the four levels in the model, in particular the location and role of Si-O bonds, vi) a theoretical prediction for all the main parameters of the four level model.

4. Er coupled Silicon nanocrystals

The recent increase in the transmission capacity of the fibre optic based communication link is also related to the availability of all-optical amplifiers based on Er doped fibres.[37] In this amplifier, a silica optical fibre is doped with Er^{3+} ions, whose internal atomic-like transition at 1.54 μm is exploited to achieve light amplification. In the past, several attempts have been done to reproduce a similar materials system in silicon.[38] Several breakthroughs have been recently achieved in the field of Er doping of crystalline Si that allowed to fabricate LED operating at room temperature.[39-41] State-of-the-art devices have room temperature quantum efficiencies of $5x10^{-4}$ and can operate at modulation frequencies more than 10 MHz. In order to achieve room temperature operation of Er doped Si LED, Er has to be incorporated at high concentrations in Si without the formation of precipitates. The low solid solubility of Er in Si is a problem for incorporation and can be solved by the use of co-dopants (such as O or F) which, through the formation of Er-impurity complexes,

avoid Er precipitation into the optically inactive silicide phase and enhance the effective solid solubility of Er in crystalline Si. Second, it has to be incorporated in its optically active 3+ state. Then the electronic system of Si should be in contact with the Er 4*f* shell. This is needed to produce a rate of excitation through electron-hole mediated processes of the levels involved in the transition as efficient as possible. In particular the excitation process should be more efficient than competing routes of electron-hole recombination such as Auger recombination and recombination at deep levels. Finally, once excited, Er should decay radiatively. This radiative decay will be in competition with non-radiative de-excitation processes which can be extremely severe due to the long radiative lifetime of Er in Si (2 ms). By using co-ion-implantation of Er and O and annealing treatments, all these issues have been positively faced and high efficiency LED have been produced.[39-41]

What it is more interesting for light amplification studies is the experimental finding of a strong enhancement of the Er luminescence when Er is implanted or deposited in a SiO_2 matrix where Si-nc have been formed,[42-44] i. e. Si-nc acts as sensitizers for erbium ions. Non-radiative de-excitation processes are reduced by widening the Si bandgap and thus avoiding one of the most detrimental sources of Er luminescence quenching.[38] Indeed the thermally activated back-transfer of excitation from Er^{3+} to Si-nc becomes less efficient than in bulk Si since the energy mismatch for the process becomes larger. Widening of the band gap also produces a reduction in the free carrier concentration thus limiting the Auger process. As demonstrated in Fig. 14, the strong luminescence comes from Er ions that are pumped through an electron-hole mediated process in which photo-excited excitons from Si nanocrystals transfer their energy to Er ions in a fashion similar to what shown for single crystal Si. The number of Si-nc coupled to a single Er ion is still a debated issue (between 1 to 10).[42,44] As what concerns where Er is placed, from high resolution luminescence it is clear that most of the Er is in the SiO_2 matrix, which is an ideal situation if one looks at reproducing the environment which is found in Er doped fibre amplifier. Hence, Er coupled Si-nc benefits of the advantages of both silicon (efficient excitation) and SiO_2 (weak non-radiative processes, i. e. negligible temperature quenching of the luminescence), while it avoids their disadvantages (low excitation efficiency in SiO_2 and strong non-radiative processes in bulk Si). Indeed MOS light emitting devices operating at room T have been made with this system, where it is demonstrated a quantum efficiency larger than 1%.[45] Even higher efficiencies (10%) are reported for Er in silicon rich oxide films, however in this system reliability is still an issue.[46]

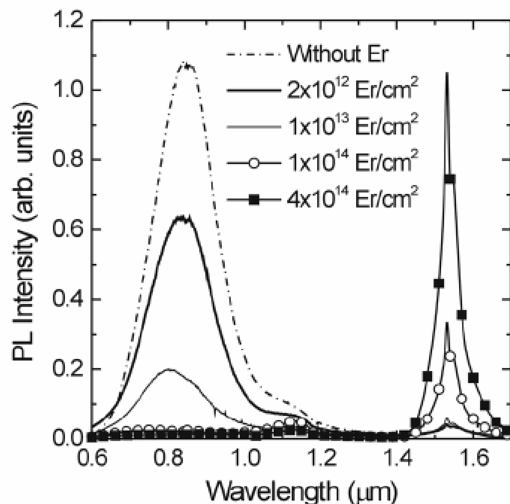

Figure 14. Room temperature PL spectra of Er-implanted Si nanocrystals at different Er doses. The pump power of the laser beam was 50 mW. After ref. 42.

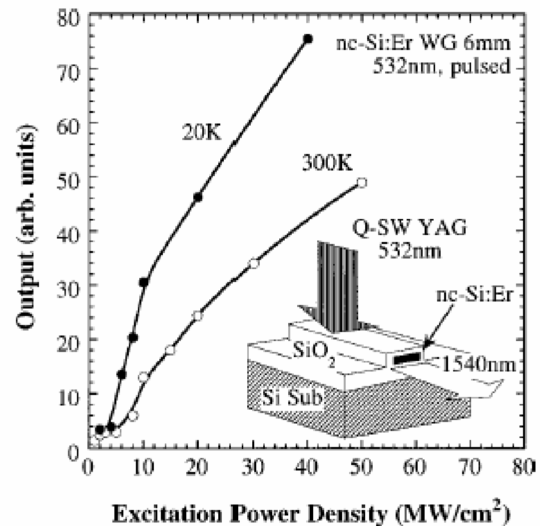

Figure 15. Pumping power density dependence of the 1540 nm emission of a 6 mm Er-doped nc-Si waveguide. After ref. 47

The layer co-doped with Si-nc and Er^{3+} ions has a refractive index which is larger that SiO_2, i. e. waveguides can be formed where Er^{3+} coupled to Si-nc is contained in the core. Experiments have shown that luminescence increases (Fig. 15) or even evidences of signal enhancement (Fig. 16) are present in these waveguides. This last result is very interesting and was confirmed also by experiments we performed in my laboratory.[50] The technique used in Ref. 48 was a true

pump and probe measurements in waveguide configuration. Even though no net optical gain was measured, an enhancement in the probe transmission at 1.535 μm was observed as the pump power is increased. By rather crude approximations,[48] it is possible to write that the probe transmission when the pump is on I(P) is related to the probe transmission when the pump is off I(0) by $SE \equiv I(P)/I(0) = \exp(2(\sigma N_2\Gamma)L)$, where SE is the signal probe enhancement, σ is the Er^{3+} emission cross section at 1.535 mm, N_2 the density of excited Er ions, Γ the optical mode confinement factor and L the waveguide length. A fit of the experimental data yields an increased Er^{3+} emission cross section with respect to Er ions in silica or in silicon. This is a quite unexpected results, which has been however confirmed by other research groups.[44,50] The reason is still unclear, one can speculate about the role of the dielectric environment which is modified by the presence of the Si-nc.[44] What makes this finding interesting is the possibility to significantly reduce the cavity length in an amplifier or laser than the one usually employed in the silica doped fiber systems. To summarize the very interesting properties of the Er^{3+} coupled Si-nc system, Table 2 compares the main cross sections of Er^{3+} in silica, silicon and coupled with Si-nc.

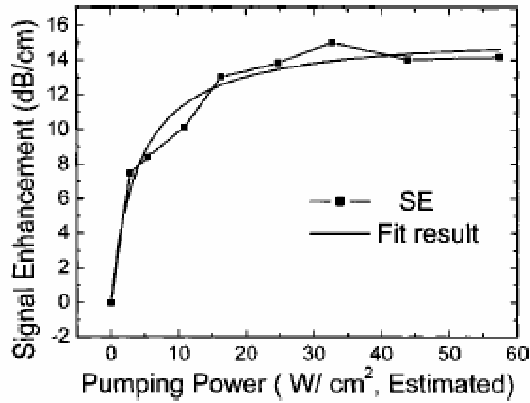

Figure 16. Pump power dependence of the signal enhancement SE and of a theoretical fit. A SE of up to 14 dB/cm, implying a possible net gain of up to 7 dB/cm, is found. From the fit, an emission cross section of $2x10^{-19}$ cm^2 and an effective excitation cross section of $>10^{-17}$ cm^2 at 477 nm was a deduced From Ref. 48.

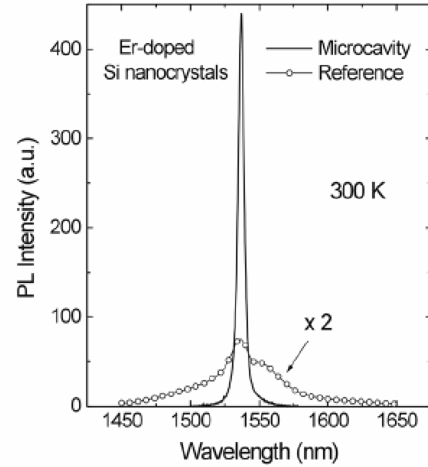

Figure 17. Room temperature PL spectra for an Er-doped Si nanocrystals microcavity (continuous line). The spectrum of Er-doped Si nanocrystals outside the cavity is also shown for comparison (circles). After Ref. 32.

TABLE 2 Summary of the various cross sections related to Er^{3+} in various materials.

	Er in SiO_2 (cm^2)	Er in Si (cm^2)	Er in Si-nc (cm^2)	Reference for Er in Si-nc
Effective excitation cross section of luminescence at a pumping energy of 488 nm	$1\text{-}8x10^{-21}$	$3x10^{-15}$	$1.1\text{-}0.7x10^{-16}$	51,52
Effective excitation cross section of electroluminescence		$4x10^{-14}$	$1x10^{-14}$ by impact ionization	45
Emission cross section at 1.535 μm	$6x10^{-21}$		$2x10^{-19}$	53,50
Absorption cross section at 1.535 μm	$4x10^{-21}$	$2x10^{20}$	$8x10^{-20}$	54

The system Er^{3+} coupled to Si-nc is very promising for laser applications because the active material (Er^{3+} in SiO_2) has already shown lasing properties. In addition, the technology to produce the material is very compatible with CMOS processing. Microcavities with excellent luminescence properties have been also demonstrated (Fig. 17),[32] which allows designing both edge emitting or vertical emitting laser structures. The issue related to electrical pumping of the active material, which was believed to be a major short-cut of this approach, is no longer a problem as extremely high efficiency LED have been demonstrated.[45,46] The major still open issue is to engineer the waveguide losses in order to be able to measure net optical gain and not only signal enhancement in pump and probe experiment. This seems only a problem of time and research efforts.

5. Si/Ge quantum cascade structures

One route to avoid the fundamental limitations to lasing in silicon, i. e. its indirect band-gap, is to avoid using interband transition. Indeed if one exploits only intraband transition, e. g. intra valence band transition, no fundamental problems exist to impede lasing in silicon.[55] This is indeed the approach of the quantum cascade (QC) Si/Ge system, where one is trying to use the concept that was already successful in III-V semiconductors, which is advancing as a viable option for mid-IR emission, covering today a large wavelength range, 3–24 μm.[56]

The idea of the device is shown in Fig. 18. Both conduction band or valence band based QC systems can be designed. However, to achieve confinement potential in the conduction band, growth of a relaxed SiGe buffer is necessary, whereas for pseudomorphic growth on a Si substrate most of the band offset occurs in the valence band. Hence, the cascading scheme has to be implemented using holes in the valence band, in contrast to QC lasers based on III–V semiconductors that employ electron cascade structures.[56] In figure it is shown an electron-injected n-i-n conduction band device, although a hole-injected p-i-p valence band device is the one which is usually employed. The carriers make a vertical transition between subbands 3 and 2, and then they cascade down the electrically biased staircase. In order to assist population inversion, the lower laser level 2 is rapidly depopulated by phonon emission if, by design, the energy difference between levels 2 and 1 is resonant with phonon energies. Practically one has two identical active regions connected by an injector. Electroluminescence from SiGe quantum cascade structure grown on Si has recently been demonstrated.[57-60]

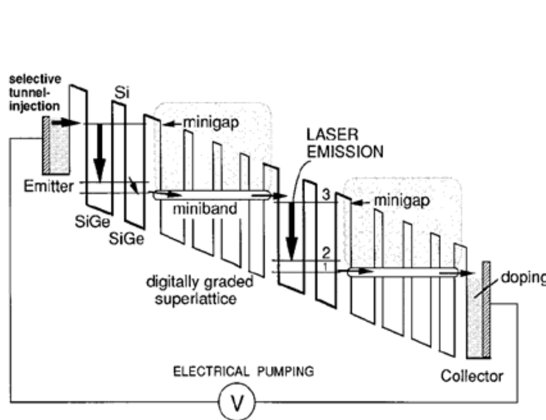

Figure 18 Silicon based intersubband quantum-cascade laser. After Ref. 55

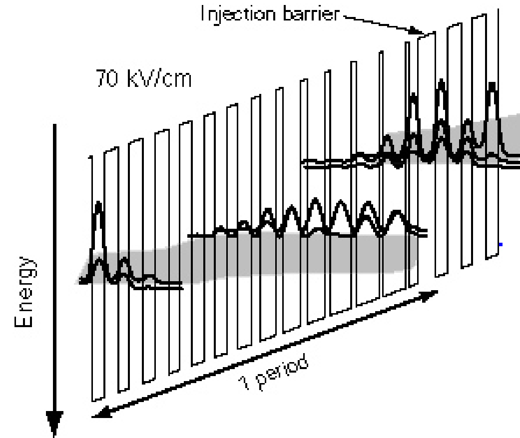

Figure 19 Schematic valence band diagram of one stage of the structure, under an applied electric field of 70 kV/cm. Only the HH band and the module squared of the relevant HH wave functions are shown for clarity. Note that the axis of the energy is turned upside down. Each period, starting from the injection barrier, consist of the following sequence of Si barrier (roman) and $Si_{0.2}Ge_{0.8}$ (bold) in Å: 25/**11**/4/**26**/5/**26**/6/**24**/7/**21**/8/**19**/9/**18**/10/**17**/<u>11</u>/<u>**15**</u>/<u>12</u>/<u>**15**</u>/<u>13</u>/<u>**14**</u>/<u>15</u>/**14**/16/**13**/17/**13**. The underlined numbers correspond to doped layers with a boron concentration of $5x10^{17}$ cm^{-3}. From Ref. 57

Starting from the possibility of monolithic integration with silicon microelectronics, the Si/SiGe system actually offers numerous advantages over III-V heterostructures for quantum cascade laser application. Due to the covalent bonding, the nonpolar phonon scattering is not interfering: the nonpolar electron-phonon interaction is the dominant loss process in III-V quantum cascade lasers. The optical phonon energy in Si is much higher than in GaAs (64meV compared with 36meV), providing a larger frequency window within which (nonpolar) optical phonon scattering is suppressed. In Si the thermal conductivity is much larger than that of GaAs, giving better prospects of CW operation at non-cryogenic temperatures. However, the SiGe on material system has several additional constraints, such as:[57] the necessity to work in the valence band and thus the higher effective masses of the charge carriers, limited band offset of approximately 80

meV per 10% Ge concentration and splitting into heavy hole (HH) and light hole (LH) bands. Moreover, the high amount of strain due to the lattice mismatch between Si and Ge, sets an upper limit to the number of wells per cascade, the number of cascades, as well as the thickness and Ge content of each individual well. Due to the mentioned constraints, the developed Si=SiGe cascade structure is a drastically simplified version of the typical III–V QC structure. As shown in Fig. 19, in a practical QC structure each cascade consists of only 4 wells.

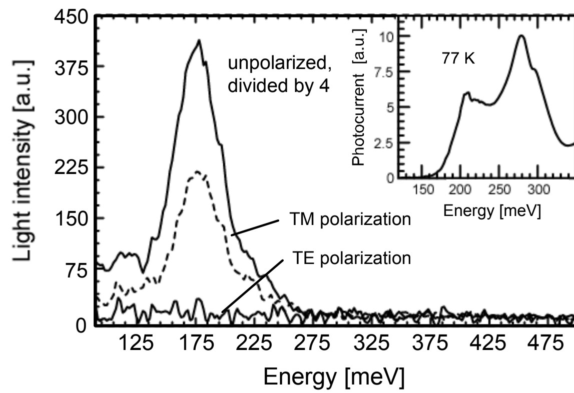

Figure 20. Electroluminescence spectra of the sample with 15 repetitions, taken at 80K with and without a polarizer placed in the light path. The parameters are 4.7 V, 550mA, 94kHz and a duty cycle of 10%. The polarized electroluminescence is measured at 5.2V, 650mA and a 20% duty cycle. The inset shows the results of a photocurrent measurement at 77K. From Ref. 60.

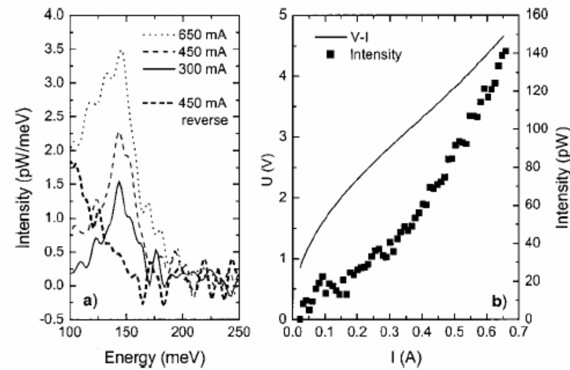

Figure 21. (a) Current-dependent EL spectra in forward bias and spectrum at reverse bias at 80K. (b) I-V curve and integrated EL intensity. From Ref. 59

Figure 20 and 21 show the typical electroluminescence spectra recorded in QC structures grown on Si substrates. The levels involved are valence levels, the radiative transition is between heavy hole states. The quantum efficiency estimate is about 10^{-5} for electroluminescence.[57-60] Temperature-dependent measurements show nearly identical spectra between 20 and 90 K and a broadening and vanishing of the peak at about 160 K. It is possible to improve these results controlling the large accumulation of strain imposed by the use of a Si substrate. This has been done using a $Si_{0.5}Ge_{0.5}$ substrate and growing on it strain compensated $Si_{0.2}Ge_{0.6}$/Si quantum wells. Intersubband transition have been observed by absorption measurements at 235, 262 and 325 meV changing the well width from 3.5 to 2.5 nm, peaks are observed up to room temperature.[60] For similar structures EL has been detected at 80 K.[60]

The QC concept is working for III-V semiconductors. SiGe system has some advantages and a fundamental limit posed on the number of periods of successive QW cascades which is given by the critical thickness for the formation of misfit dislocation. Hence, even though these devices show interesting EL properties for the prospect to the development of a Si-based laser, highly evolved cascade structures have to be realised. As the gain per single element is low due to the nature of the intraband transition, a large number of cascading structures will be needed to accumulate a macroscopic gain. In addition, all these have to be integrated within a waveguide cavity. The possible solutions may come from the use of Si-on-Insulator (SOI) substrates or thick, relaxed SiGe graded buffer.[60] No stimulated emission in SiGe QC structures has been reported to date. In addition the emission wavelength is different than those commonly used for optical interconnects. Despite some authors propose to use quantum cascade laser for free-air optical interconnects, such a Si/Ge quantum cascade laser will be of little use for Silicon photonics if all other compatible elements will be integrated such as detectors and waveguides.

6. THz emission

A gap in the frequency spectrum of electromagnetic waves opens across the THz region, where no semiconductor sources are available. At low frequencies, sources are made by electronic oscillators (high speed transistors) while at high frequencies the sources are made by injection lasers. Recently a THz laser has been demonstrated by using III-V

semiconductors which shows the way to cover this THz gap.[61] With the same aim, and using the many advantages of the SiGe system over the III-V systems for these frequencies, a research effort is spent to implement the QC concept and making a laser in these frequency regions.[62-64] The typical structure is shown in Fig. 22 which by using p-type heterostructures is designed to emit radiation from light hole – heavy hole transitions. In these way both edge emission and surface-normal THz emission might be obtained. Growth of p-Si/SiGe quantum cascade structures comprising up to 100 periods has been demonstrated using low pressure CVD via a strain-balanced approach on virtual substrates.[64] Intersubband THz electroluminescence from a range of Si/SiGe quantum cascade structures has been observed in both edge and surface-emission geometries. An example is show in Fig. 23. The light to heavy hole intersubband lifetime was measured to be ~20ps, which is over an order of magnitude longer than high temperature values in III-V heterostructures, implying that a Si/SiGe THz QC laser may be capable of much higher operating temperatures than corresponding III-V devices. Emission power levels comparable to the one reported on III-V devices before laser processing have been measured which indicate that there are good prospects for realisation of a THz Si/SiGe QCL via further optimisation of the active region and appropriate cavity design.

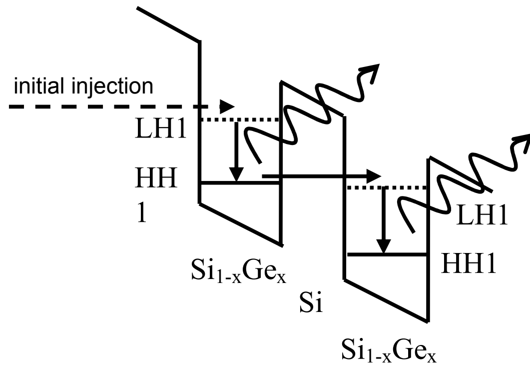

Figure 22. Schematic valence band profile of a Si/SiGe quantum staircase laser operating via radiative LH1-HH1 transitions. From Ref. 64.

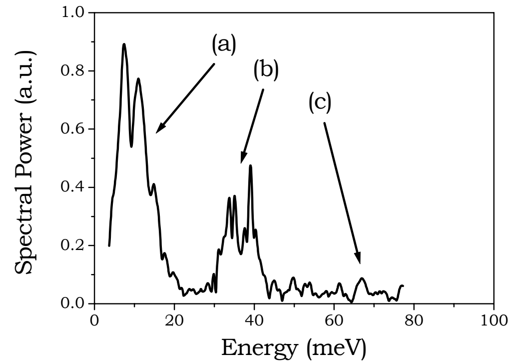

Figure 23. FTIR edge-emission spectrum for a quantum cascade structure, at a temperature of 4.2K. The pulsed bias voltage was 7 V with a 10% duty cycle. The features marked (a), (b) and (c) correspond to the theoretically calculated emission peaks for the LH1-HH1, HH2-HH1 and LH2-HH1 intersubband transitions, respectively. From Ref. 64.

Another approach to THz laser emission in silicon has been developed.[65-68] The idea is to make a THz laser using intra-shallow donor optical transitions in silicon. A band diagram showing the lasing transition is reported in Fig. 24. Very narrow spectral emission and the light intensity threshold versus pumping power are reported in Fig. 25. Despite the claims of lasing for this approach, it is not yet clear the cavity structure, the optical mode pattern and the evolution from spontaneous to stimulated emission. Other concerns for a viability of the approach are related to the dilute doping of the system in order to avoid impurity-impurity interaction which will prevent population inversion and the schemes for electrical injection.

7. CONCLUSION

In this paper I have tried to review the most recent efforts to produce a silicon laser. Even though a silicon laser has not been reported yet, the work here presented shows that many important step forwards have been accomplished these last years and that the perspectives to achieve a laser in silicon are very good.

It is a pleasure to acknowledge all the people in the Silicon Photonics research group of Trento (in particular L. Dal Negro, M. Cazzanelli, Z. Gaburro, N. Daldosso and P. Bettotti) and the financial supports of EC through the Sinergia project, of INFM through the Ramses project, of Provincia Autonoma di Trento through the Profill project. S. Ossicini, F. Priolo, F. Iacona are also thanked for valuable discussions and collaboration on this topic.

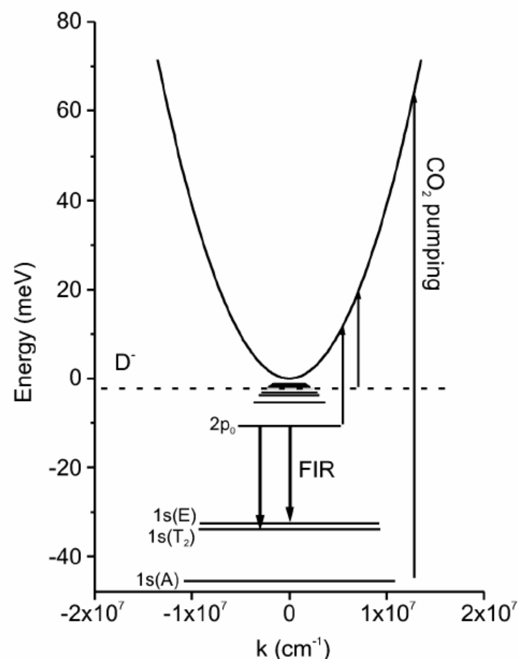

Figure 24. Optical transitions in Si:P. The dashed line represents the energy level of the D- center state. From Ref. 67

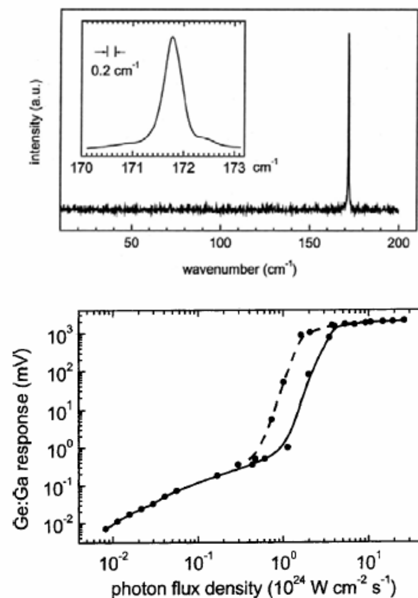

Figure 25. (top) Stimulated emission spectrum from Si:Sb. The emission line is identified with the $2p_0 \rightarrow 1s$ intracenter Sb transition. (bottom) Dependence of the emission on the pump power for 9.6 µm excitation (dashed line) or the 10.6 µm excitation (solid line). From Ref. 68

REFERENCES

1. International Technology Roadmap for Semiconductors, 2000 Update, Interconnect (http://public.itrs.net.)
2. R A Soref, *Proc. of IEEE* **81** (12 dec 1993) 1687.
3. L. C. Kimerling *Appl. Surf. Science* **159–160** (2000) 8.
4. O Bisi, S U Campisano, L Pavesi and F Priolo *Silicon based microphotonics* (IOS press, Amsterdam 1999)
5. G Masini, L Colace and G Assanto *Mat. Science Eng. B***89** (2002) 2–9
6. A Irace, G Coppola, G Breglio and A Cutulo *IEEE J. Sel. Top. Quantum Elect.* **6** (2000) 14
7. B Li, Z Jiang, X Zhang, X Wang, J Wan, G Li and E Liu A*ppl. Phys. Lett.* 74 (1999) 2108
8. S M Csutak , J D Schaub, W E Wu and J C Campbell *IEEE Photon. Technol. Lett.* **14** (2002) 516
9. S Winnerl, D Buca, S Lenk, Ch Buchal, S Mantl and D-X Xu *Mat. Science Eng. B***89** (2002) 73–76
10. B Gelloz and N Koshida *J. Appl. Phys.* **88** (2000) 4319
11. MA Green, J Zhao, A Wang, PJ Reece and M Gal *Nature* **412** (2001) 805
12. *Towards the first silicon laser*, edited by L. Pavesi, S. Gaponenko and L. Dal Negro, NATO Science Series (Kluwer Academic Publishers, Dordrecht 2003)
13.
14. W.L. Ng, M.A. Lourenço, R.M Gwilliam, S. Ledain, G. Shao and K.P Homewood *Nature* **410** (2001) 192-194.
15. W P Dumke Phys. Rev. **127** (1962) 1559
16. O. Gusev, M. Bresler, I. Yassievich, B. Zakharchenya *Efficient electroluminescence in alloyed silicon diodes* in Ref. 12 pag. 21.
17. David Sotta "*Milieux emetteurs de lumiere et microcavites optique en silicium monocristallin sur isolant*", Thesis Specialite physique, Universite Joseph Fourier Grenoble I (Grenoble, France 2002)
18. P. Jonsson, H. Bleichner, M. Isberg, and E. Nordlander *J. Appl. Phys.* **81** (1997) 2256
19. L. T. Canham, *Appl. Phys. Lett.* **57** (1990) 1046.
20. O. Bisi, S. Ossicini and L. Pavesi, Surface Science Reports **264** (2000) 1-126.
21. M. Zacharias, et al. *Silicon technology used for size-controlled silicon nanocrystals* in Ref. 12 pag. 131
22. L Pavesi, L Dal Negro, C Mazzoleni, G Franzò and F Priolo *Nature* **408** (2000) 440
23. L. Dal Negro, et al. *Stimulated emission in plasma enhanced chemical vapour deposited silicon nanocrystals*, Physica E (2003).

24. L Khriachtchev, M Rasanen, S Novikov, J Sinkkonen *Appl. Phys. Lett.* **79** (2001) 1249
25. M H Nayfeh, et al. *Appl. Phys. Lett*. **78** (2001) 1131
26. M H Nayfeh, S Rao, N Barry *Appl.Phys. Lett.* **80** (2002) 121
27. K. Luterova, et al. *J. Appl. Phys.* **91** (2002) 2896
28. Philippe M. Fauchet and Jinhao Ruan, *Optical amplification in nanocrystalline silicon superlattices* in Ref. 12 pag. 197.
29 M. Ivanda, et al. *Experimental observation of optical amplification in silicon nanocrystals*, in Ref. 12 pag. 191.
30. L. Dal Negro, et al. *Stimulated emission in silicon nanocrystals* in ref. 12 pag. 145
31. J.Valenta, I. Pelant, J. Linnros *Appl. Phys. Lett*. **81** (2002) 1396
32. F Icona, G Franzò, EC Moreira, F Priolo *J. Appl. Phys.* **89** (2001) 8354
33. A review is in Z. Gaburro and L. Pavesi *Light Emitting Diodes for Si Integrated Circuits* in *Handbook of luminescence, Display Materials, and Nanocomposites* Edited by H. S. Nalwa and L. S. Rohwer (American Scientific Publishers, 2003)
34. G Franzò, et al. *Appl. Phys*. **A74** (2002) 1
35. Ching-Fuh Lin, Peng-Fei Chung, and Miin-Jang Chen Wei-Fang Su *Optics Lett.* **27** (2002) 713
36. Heikkila L, T. Kuusela T, Hedman HP *Superl. Microstructures* **26** (1999) 157
37. P. C. Becker, N. A. Olsson, J. R. Simpson *Erbium-doped Fibre Amplifiers* (Academic Press, London 1999)
38 F. Priolo Light emission of Er^{3+} in crystalline silicon in Ref. 4 pag. 279; A. Polman, Erbium implanted thin film photonic materials, *J. Appl. Phys.* 82, 1 (1997).
39 G. Franzò, F. Priolo, S. Coffa, A. Polman, and A. Carnera, *Appl. Phys. Lett.* 64, 2235 (1994).
40 S. Coffa, G. Franzò, and F. Priolo, *Appl. Phys. Lett.* **69** (1996) 2077
41 S. Coffa, G. Franzò, F. Priolo, A. Pacelli, and A. Lacaita, *Appl. Phys. Lett.* **73** (1998) 93
42 G. Franzò, V. Vinciguerra, F. Priolo *Appl. Phys.* **A69** (1999) 3; G. Franzo, et al, *Appl. Phys. Lett.* **76** (2000) 2167.
43 M. Zacharias, et al., *Physica E* **11** (2001) 245.
44 Pieter G. Kik and Albert Polman Towards *an Er-doped Si nanocrystal sensitized waveguide laser* in Ref. 12 pag. 383
45 F. Iacona, at al. *Appl. Phys. Lett.* **81** (2002) 3242
46 M. E. Castagna, S. Coffa, L. Carestia, A. Messian, C. Buongiorno, Proceedings of ESSDERC (Bologna 2002).
47. Xinwei Zhao, Shuji Komuro, Hideo Isshiki, Yoshinobu Aoyagi, and Takuo Sugano *Appl. Phys. Lett.* **74** (1999) 120
48 Jung H. Shin, Hak-Seung Han and Se-Young Seo *Optical gain using nanocrystal sensitized Erbium* in Ref. 12 pag. 401
50 L. Dal Negro, et al. Enhanced emission cross section and vsl analysis of erbium coupled silicon nanocrystals to be published.
51 F. Priolo, G. Franzo, D. Pacifici, V. Vinciguerra, F. Iacona, and A. Irrera, *J. Appl. Phys.* **89**, (2001) 264
52 A. J. Kenyon, et al. *J. Appl. Phys* **91** (2002) 367
53 Hak-Seung Han, Se-Young Seo, Jung H. Shin, Namkyoo Park *Appl. Phys. Lett.* **81** (2002) 3720
54 P. G. Kik and A. Polman, *J. Appl. Phys.* **91** (2002) 534
55. R. A. Soref, *Thin Solid Films* **294** (1997) 325
56 C Gmachl, F Capasso, DL Sivco, et al. *Rep Prog Phys* **64** (2001) 1533-1601
57 G. Dehlinger, et al. *Materials Science and Engineering* **B89** (2002) 30–35
58 L. Diehl, et al. *Appl. Phys. Lett.* **81** (2002) 4700
59 K Bormann, et al. *Appl. Phys. Lett.* **80** (2002) 2260
60 L. Diehl, et al. *Strain compensated Si/SiGe quantum cascade emitters grown on SiGe pseudosubstrates* in Ref. 12 pag. 325
61 R Kohler, A Tredicucci, F Beltram, H Beere, E Linfield, G Davies, and D Ritchie, R C Iotti and F Rossi, *Nature* **417** 156 (2002)
62 S. A. Lynch, et al. *Appl. Phys. Lett.* **81**(2002)1543
63. S.A. Lynch, et al. *Materials Science and Engineering* **B89** (2002) 10–12
64 R. W. Kelsall, et al. Ter*ahertz emission from Silicon-Germanium quantum cascade* in Ref. 12 pag. 367
65 S. G. Pavlov, et al. *Terahertz silicon laser: Intracenter optical pumping* in Ref. 12 pag 331; V. N. Shastin, et al. *Silicon lasers based on shallow donor centers Theoretical background and experimental results* in Ref. 12 pag. 341
66 N. Shastin, et al. *Appl. Phys. Lett.* **80** (2002) 3512
67 A. Blom, M. A. Odnoblyudov, H. H. Cheng, I. N. Yassievich, K. A. Chao *Appl. Phys. Lett.* 79 (2001) 713
68 S. G. Pavlov, et al., *Phys. Rev. Lett.* **84** (2000) 5220; S. G. Pavlov, et al. *J. Appl. Phys.* **92** (2002) 5632